Lumped Parameter Model of Cockcroft-Walton Voltage Multiplier in Resonant Converters

Seong-Ho Son[1], Tae-Hyun Kim[1], Chang-Hyun Kwon[1],
Sung-Roc Jang[1,2], Chan-Hun Yu[1], Hyoung-Suk Kim[1,2]

[1] University of Science and Technology (UST), South Korea
[2] Korea Electrotechnology Research Institute (KERI), South Korea

***Abstract*-- This paper proposes a lumped parameter model for Cockcroft-Walton voltage multiplier (CWVM) circuits in resonant converters. The proposed model converts the CWVM circuits to ideal rectifiers and two lumped capacitors. This can reduce the analysis error caused by the resonance between the resonant inductors and CWVM capacitors. Also, the number of converter components can be reduced by utilizing the lumped capacitors as resonant capacitors. The accuracy and applicability of the proposed model are demonstrated through PSIM simulation. For the practical use of the proposed model, the design and implementation of an LCC resonant converter, which is suitable for high step-up applications, are presented. The experimental results from the 5kW and 10kV LCC resonant converter are shown to verify the proposed works.**

***Index Terms*--Voltage multiplier, Resonant converter, High voltage power supply.**

I. Introduction

Cockcroft-Walton voltage multiplier (CWVM) circuits are widely used in many high voltage power supplies (HVPSes) due to their high voltage gain, low voltage stress of components, and circuit simplicity [1]-[7]. According to the output voltage, output current, and operating frequency, various configurations can be utilized as shown in Fig. 1.

For the HVPSes, resonant converters are proper candidates to adopt the CWVM as a rectifier because they can reduce the voltage drop of CWVM by increasing the switching frequency due to their soft switching capability [3]-[7]. Among many resonant converters, three element topologies are widely used in many industrial applications because they have many advantages in the view of circuit simplicity, load range, size, and cost. Compared with an LLC resonant converter, an LCC resonant converter is more suitable to use the CWVM as the rectifier since it can utilize the parasitic components of the high voltage transformer and CWVM as the resonant tank [5]-[7].

When CWVMs are utilized as the rectifiers in the resonant converter, they show voltage drop according to the output current, operating frequency, the number of stages, and capacitance constituting the CWVM [8]. In addition, the CWVM capacitors resonate with the resonant inductors. Since this affects the voltage gain and resonant current of converter, the analysis errors are increased and changed according to the operating conditions [6], [7]. Therefore, a lot of trials and errors are required to design the resonant converters with CWVM. Although several papers have been published to analyze the CWVM voltage drop [8]-[10], the resonance between the resonant inductor

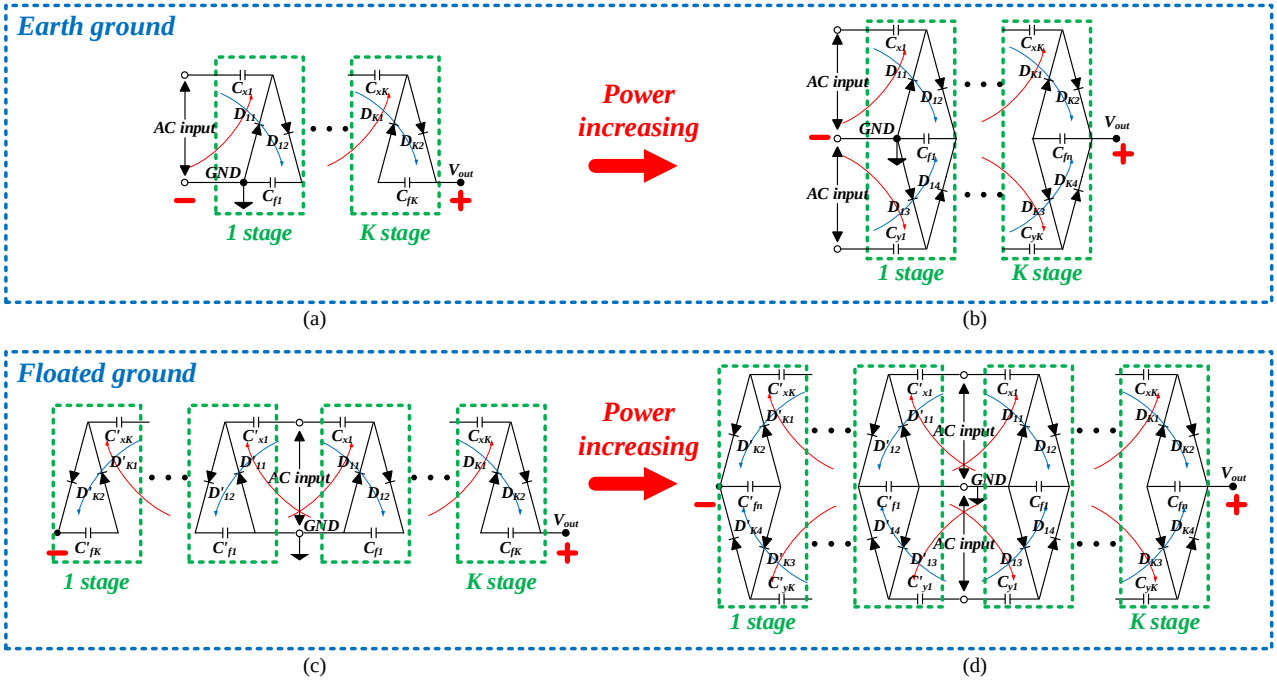

Fig. 1. Configurations of CWVM. (a) Half-wave CWVM. (b) Full-wave CWVM. (c) Bipolar half-wave CWVM. (d) Bipolar full-wave CWVM.

and CWVM capacitors are not considered because they assume that the front-end inverter as an ideal sinusoidal voltage source. To analyze the resonant converter with CWVM, several methods are presented. In [6], a unified model for the LCC resonant converter with CWVM circuits is proposed. It consider the junction capacitor of CWVM as well as the voltage drop of CWVM. However, the resonance occurred by CWVM capacitors is not addressed. In [7], even though the scheme converting the CWVM into two capacitors and ideal full-wave rectifier is proposed, it only deals with bipolar full-wave CWVM for high power HVPSes.

To solve abovementioned problems, a lumped parameter model is proposed for the resonant converter with CWVM. Since this model converts the CWVM to the ideal rectifiers and two lumped capacitors according to the CWVM configurations, the resonance between resonant inductors and CWVM capacitors can be analyzed with small error by absorbing the lumped capacitors into the resonant tank. In addition, the number of resonant components can be reduced by utilizing the two lumped capacitors as resonant capacitors. To verify the accuracy of the proposed model, comparisons with the actual CWVM and the proposed model are presented through PSIM simulation. Also, to confirm the applicability of the proposed model in resonant converters, the experimental results from a 10kV and 5kW LCC resonant converter are provided.

II. Proposed Lumped Parameter Model of CWVM

As shown in Fig. 1, various configurations of CWVM can be adopted according to the output power, switching frequency, and ground of resonant converter. For the proposed lumped parameter model, the half-wave CWVMs shown in Fig. 1(a) and Fig. 1(c) are replaced by an ideal half-bridge rectifier and two lumped capacitors (C_{eqs} and C_{eqp}), and the full-wave CWVMs shown in Fig. 1(b) and Fig. 1(d) are converted into an ideal full-bridge rectifier, C_{eqs} and C_{eqp}. Bipolar CWVMs shown in Fig. 1(c) and Fig. 1(d) can be adopted if the application ground can be floated. Since the operation is similar to unipolar CWVMs except that the power is transferred in both directions, only the model for unipolar CWVMs is derived. To simplify the derivation, five assumptions (A_1-A_5) are made as follows:

A_1. CWVMs have large output filter capacitor (C_o), so that the output voltage (V_o) and output current (I_o) of CWVMs are considered as constant.

A_2. All parasitic components except the junction capacitors (C'_{jK4}-C_{jK4}) of diodes (D'_{1K}-D_{4K}) are neglected.

A_3. The values of the oscillation capacitors (C'_{xK}-C_{yK}) and the filter capacitors (C'_{fK}-C_{fK}) are the same as C_{CWVM}.

A_4. The capacitance of C'_{jK4}-C_{jK4} is C_{Dj}.

A_5. C_{CWVM} are sufficiently larger than C'_{jK4}-C_{jK4}.

A. Lumped Parameter Model for Half-Wave CWVMs

Fig. 2(a) shows the unipolar half-wave CWVM (HW-CWVM). To conduct the diodes (D_{11}-D_{K2}) in the HW-CWVM, C_{j11}-C_{jK2} should be charged or discharged. In this

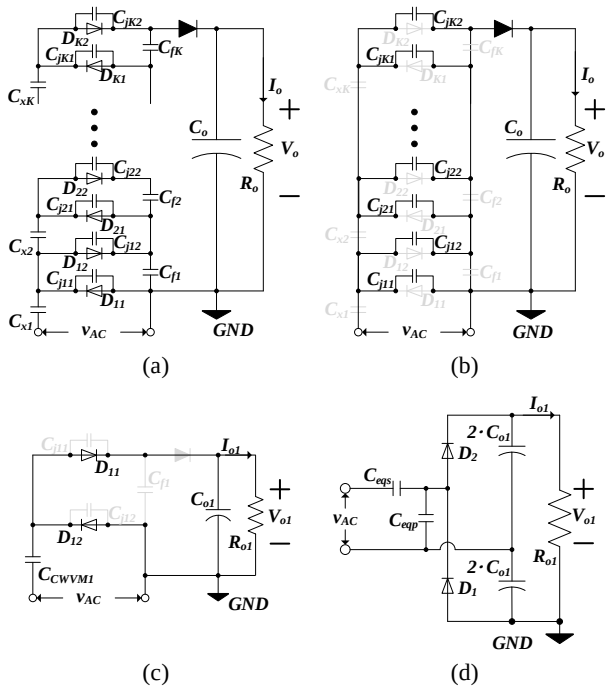

Fig. 2. Proposed modeling for half-wave CWVM. (a) Half-wave CWVM with junction capacitors. (b) Model for commutation interval of CWVM diodes. (c) 1stage half-wave CWVM. (d) Proposed model for half-wave CWVM.

case, C_{j11}-C_{jK2} can be considered as the parallel connected capacitors as shown in Fig. 2(b) since C_{x1}-C_{xK} and C_{f1}-C_{fK} are regarded as short circuit by A_4. Thus, the parallel lumped capacitor (C_{eqp}) can be expressed as follows:

$$C_{eqp} = 2 \cdot K \cdot C_{Dj} \tag{1}$$

where C_{Dj} is capacitance of C_{j11}-C_{jK2} and K is the number of stages in HW-CWVM.

The lumped series capacitor (C_{eqs}) can be derived from C_{x1}-C_{xK} and C_{f1}-C_{fK}. To obtain C_{eqs}, the HW-CWVM shown in Fig. 2(a) is firstly replaced by the 1 stage HW-CWVM shown in Fig. 2(c). Since the charges for charging and discharging C_{j11}-C_{jK2} are sufficiently small from A_4, C_{j11}-C_{jK2} are neglected in the HW-CWVM conversion. For the 1 stage HW-CWVM, the output voltage (V_{o1}) and output current (I_{o1}) can be assumed as

$$V_{o1} = \frac{V_o}{K} \tag{2}$$

$$I_{o1} = K \cdot I_o \tag{3}$$

When the load resistance of CWVM is assumed as R_o, the load resistance (R_{o1}) of 1 stage HW-CWVM can be written from (1) and (2) as follows:

$$R_{o1} = \frac{V_{o1}}{I_{o1}} = \frac{V_o}{K^2 \cdot I_o} = R_o / K^2 \tag{4}$$

Since the HW-CWVM has voltage drop (V_{drop}) according to the load current (I_o), the operating frequency (f_s), the number of stages (K), and the capacitance of HW-CWVM capacitors (C_{CWVM}), V_{drop} and V_o can be calculated as follows [10]:

$$V_o = 2 \cdot K \cdot V_{ac} - V_{drop} \tag{5}$$

$$V_{drop} = \frac{2K^3 + K}{3} \cdot \frac{I_o}{C_{CWVM} \cdot f_s} \tag{6}$$

where V_{ac} is AC input voltage of HW-CWVM.

By substituting the values of 1 stage HW-CWVM into (6), the voltage drop (V_{drop1}) of 1 stage HW-CWVM can be calculated as follows:

$$V_{drop1} = \frac{I_{o1}}{C_{CWVM1} \cdot f_s} \tag{7}$$

where C_{CWVM1} is capacitance of 1 stage HW-CWVM capacitors (C_{x1} and C_{f1}). To satisfy (2) and (3), the output voltage (V_{o1}) of 1 stage HW-CWVM can be expressed as follows:

$$V_{o1} = \frac{2 \cdot K \cdot V_{ac} - V_{drop}}{K} = \ 2 \cdot V_{ac} - \frac{V_{drop}}{K} \tag{8}$$

From (8), the voltage drop (V_{drop1}) of 1 stage HW-CWVM can be written as

$$V_{drop1} = \frac{V_{drop}}{K} = \frac{2 \cdot K^2 + 1}{3} \cdot \frac{I_o}{C_{CWVM} \cdot f_s} \tag{9}$$

From (7) and (9), C_{CWVM1} is derived as follows:

$$C_{CWVM1} = \frac{3 \cdot K}{2 \cdot K^2 + 1} C_{CWVM} \tag{10}$$

Since the output filter capacitor (C_{o1}) of 1 stage HW-CWVM is large enough by A_1, C_{CWVM1} can be regarded as a capacitor (C_{eqs}) connected in series to the input source, and C_{f1} can be neglected due to the parallel connection with C_{o1}. Therefore, the 1 stage HW-CWVM shown in Fig. 2(c) can be converted as the ideal half-bridge rectifier, C_{eqs}, and C_{eqp} as shown in Fig. 2(d).

B. Lumped Parameter Model for Full-Wave CWVMs

Fig. 3(a) shows the unipolar full-wave CWVM (FW-CWVM). The model for the FW-CWVM can be derived similarly to the HW-CWVM. As shown in Fig. 3(b), the diode junction capacitors (C_{j11}-C_{jK4}) can be considered as the series and parallel connected capacitors. Thus, the parallel lumped capacitor (C_{eqp}) can be expressed as (11).

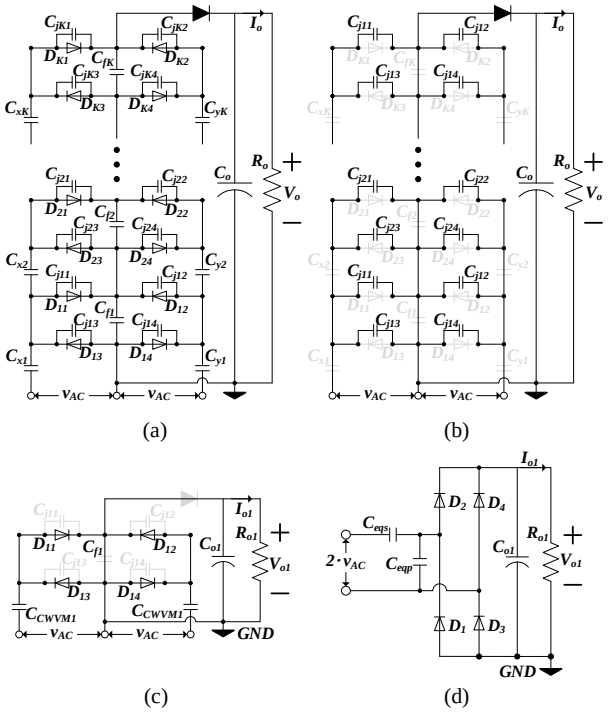

Fig. 3. Proposed modeling for full-wave CWVM. (a) Full-wave CWVM with junction capacitors. (b) Model for commutation interval of CWVM diodes. (c) 1 stage full-wave CWVM. (d) Proposed model for full-wave CWVM.

$$C_{eqp} = K \cdot C_{Dj} \tag{11}$$

where C_{Dj} is capacitance of C_{j11}-C_{jK4}.

To obtain C_{eqs}, the FW-CWVM shown in Fig. 3(a) is firstly replaced by the 1 stage FW-CWVM shown in Fig. 3(c). From [10], the output voltage (V_o) and voltage drop (V_{drop}) of FW-CWVM are calculated as (12) and (13), respectively.

$$V_o = 2 \cdot K \cdot V_{ac} - V_{drop} \tag{12}$$

$$V_{drop} = \frac{K \cdot (K+1) \cdot (2 \cdot K + 1)}{12} \cdot \frac{I_o}{C_{CWVM} \cdot f_s} \tag{13}$$

From (12) and (13), C_{CWVM1} is derived as (14) in similar way to (7)-(10).

$$C_{CWVM1} = \frac{6 \cdot K}{(K+1) \cdot (2 \cdot K + 1)} C_{CWVM} \tag{14}$$

Since C_{CWVM1} can be regarded as two capacitors connected in series to the input source due to the large C_{o1}, C_{eqs} is expressed as follows:

$$C_{eqs} = \frac{C_{CWVM1}}{2} \tag{15}$$

Therefore, the 1 stage FW-CWVM shown in Fig. 3(c) can be converted as the ideal full-wave rectifier, C_{eqs}, and C_{eqp} shown in Fig. 3(d). In this case, the input voltage of converted full-wave rectifier with C_{eqs} and C_{eqp} is $2 \cdot v_{ac}$ because the two input voltages of FW-CWVM are added.

C. Simulation results

The derived model is summarized in Table I, which includes the bipolar CWVMs. The purpose of the proposed model is to predict the resonance between the resonant inductors and CWVM capacitors. This makes it possible to obtain accurate relations in the voltage gain, resonant current, and component stress in resonant converters with

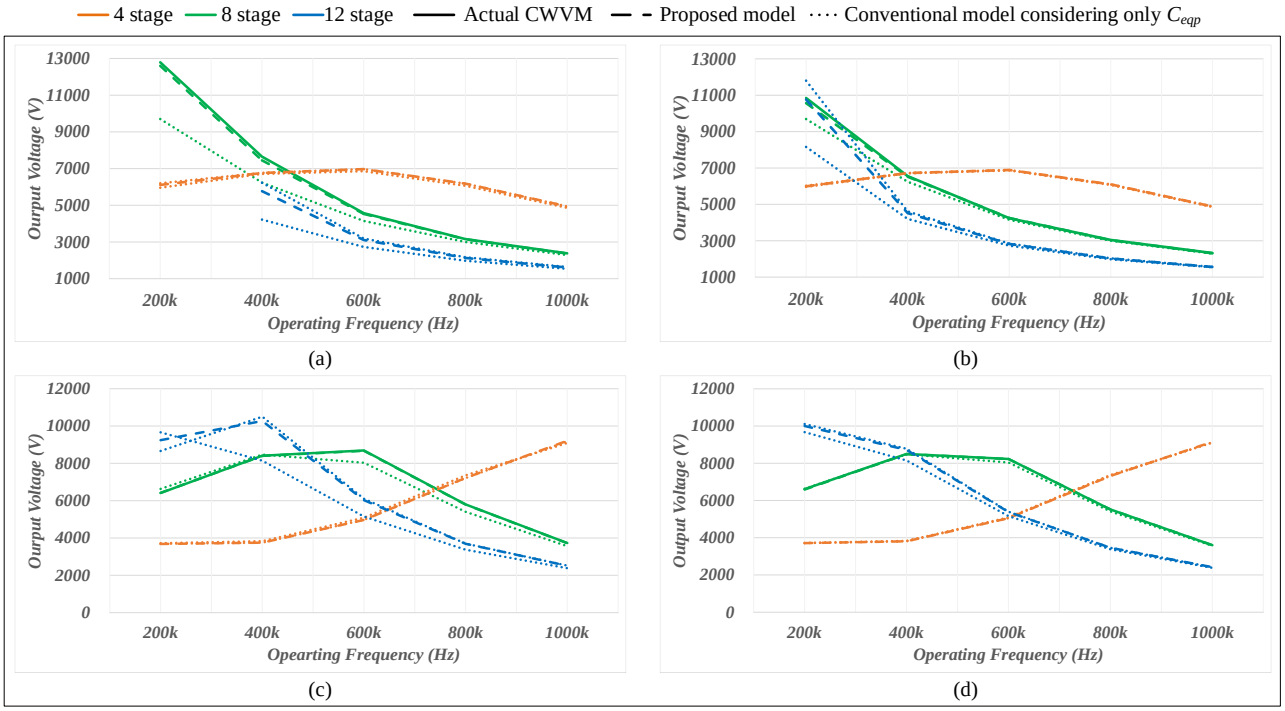

Fig. 4. Simulation results of proposed model. (a) HW-CWVM. (b) FW-CWVM. (c) Bipolar HW-CWVM. (d) Bipolar FW-CWVM.

the CWVM. For the verification, the PSIM simulation of the proposed model and actual CWVM are conducted under various conditions such as the operating frequency and the number of stages (K). The simulation results are presented in Fig. 4. The solid line is the simulation results of the actual CWVMs. The dashed line and dotted line shows the simulation results of the proposed model which includes C_{eqs} and C_{eqp} and the conventional model considering only C_{eqp}, respectively. The circuits are fed by the ideal sinusoidal voltage source of 1kV with inductor of 50uH. The junction capacitors of CWVM diode are assumed as 40pF, and the load resistance is assumed as 20kΩ. In the equivalent circuits, V_o is calculated as K times the estimated V_{o1} by (2).

TABLE I
SUMMARY OF PROPOSED MODEL FOR CWVM

	Half-Wave (Fig. 1(a))	**Full-Wave (Fig. 1(b))**
Rectifier	Half-Bridge	Full-Bridge
Output Voltage (V_{o1})	V_o/K	
Output Current (I_{o1})	$I_o \cdot K$	
Load Resistance (R_{o1})	R_o/K^2	
Parallel Lumped Capacitor (C_{eqp})	$2 \cdot C_{Dj} \cdot K$	$C_{Dj} \cdot K$
Series Lumped Capacitor (C_{eqs})	$\frac{6 \cdot K \cdot C_{CWVM}}{(4 \cdot K - 1) \cdot (K + 1)}$	$\frac{3 \cdot K \cdot C_{CWVM}}{(K + 1) \cdot (2 \cdot K + 1)}$
	Bipolar Half-Wave (Fig. 1(c))	**Bipolar Full-Wave (Fig. 1(d))**
Rectifier	Half-Bridge	Full-Bridge
Output Voltage (V_{o1})	V_o/K	
Output Current (I_{o1})	$I_o \cdot K$	
Load Resistance (R_{o1})	R_o/K^2	
Parallel Lumped Capacitor (C_{eqp})	$2 \cdot C_{Dj} \cdot K$	$C_{Dj} \cdot K$
Series Lumped Capacitor (C_{eqs})	$\frac{12 \cdot K \cdot C_{CWVM}}{(2 \cdot K - 1) \cdot (K + 2)}$	$\frac{6 \cdot K \cdot C_{CWVM}}{(K + 1) \cdot (K + 2)}$

As shown in Fig. 4, when K and f_s are large, the output voltages of both equivalent circuits are similar to the output voltages of actual CWVM. However, as K and f_s are decreased, the output voltage errors of the model considering only C_{eqp} are increased significantly. On the other hand, the proposed model keeps the small output voltage errors.

III. DESIGN AND IMPLEMENTATION OF LCC RESONANT CONVERTER WITH CWVM

A. Design of LCC Resonant Converter with CWVM

In this section, the design and implementation for the LCC resonant converter with CWVM are provided as an example to utilize the proposed model. The converter specifications are listed in Table II. From the specifications, the FW-CWVM is selected as the rectifier. The number of CWVM stage (K) is obtained as follows:

$$K = \frac{V_o}{\eta_{CWVM} \cdot V_{sec}} \tag{16}$$

where V_{sec} is the output voltage of transformer secondary side, and η_{CWVM} is the conversion efficiency of FW-

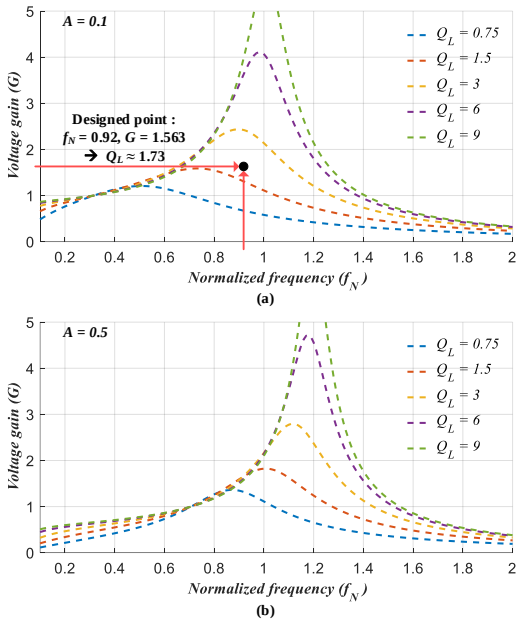

Fig. 5. G according to f_N with various A and Q_L. (a) A = 0.1. (b) A = 0.5.

CWVM. V_{sec} can be chosen as 1.5kV by considering the transformer size and the insulation material of transformer bobbin. In general, since η_{CWVM} is selected from 0.8 to 0.9 [6], K is determined as 8, and C_{CWVM} can be calculated as about 100nF from (5) and (6). The designed FW-CWVM can be converted as the full-bridge rectifier with C_{eqs} and C_{eqp} by the proposed method. Therefore, the converter can be designed based on the full-bridge rectifier with the following specifications :

$$V_{o1} = \frac{V_o}{K} = \frac{10kV}{8} = 1.25kV \quad (17)$$

$$I_{o1} = K \cdot I_o = 8 \cdot 0.5A = 4A \quad (18)$$

TABLE II
KEY PARAMETERS OF DESIGNED CONVERTER

Input voltage, V_{in}	500 Vdc
Maximum output voltage, $V_{o,max}$	10kV
Maximum output power, $P_{o,max}$	5kW
Minimum switching frequency	370kHz
Transformer turns ratio, N_{tr}	25: 40
Total number of FW-CWVM stages, K	8
Series resonant inductor, L_s	28uH
Series resonant capacitor, C_s	40nF
Parallel resonant capacitor, C_p	5.6nF
SVM capacitors, C_{x1}-C_{xK}&C_{f1}-C_{fK}	100nF

$$R_{o1} = \frac{R_o}{K^2} = \frac{20k\Omega}{8^2} = 312.5\Omega \quad (19)$$

For the design of converter, the voltage gain and stresses of components should be analyzed. A fundamental harmonic approximation (FHA) is a general solution, which replace the voltage and current of converter with their fundamental components to simplify the original circuit [11], [12]. Among many FHA for LCC resonant converter, the simple technique proposed in [11] is applied.

Fig. 5 shows the voltage gain (G) of LCC resonant converter according to normalized frequency (f_N) with various capacitance ratio (A) and quality factor (Q_L). These parameters are defined as follows:

$$f_N = \frac{f_s}{f_{op}};\ A = \frac{C_p}{C_S}; Q_L = \frac{R_{pri}}{Z_{op}} \quad (20)$$

where f_s is the switching frequency, f_{op} is the resonant frequency of series resonant inductor (L_s) and parallel resonant capacitor (C_p), C_s is series resonant capacitor, R_{pri} is the load resistor reflected to the transformer primary side, and Z_{op} is characteristic impedance of L_s and C_p. As shown in Fig. 5, when A or Q_L increases, the magnitude and slope of G increase. These indicates that the transformer turns ratio (N_{tr}) can reduced and the output voltage can be regulated with small frequency variation. However, large A and Q_L causes increased power losses and inductor size [6]. Thus, A, Q_L, and G should be selected by considering this trade-off. From the selected resonant parameters, N_{tr} is obtained as

$$N_{tr} = \frac{V_{o1}}{V_{in} \cdot G} \quad (21)$$

For the converter, A, Q_L and G are designed as about 0.14, 1.73, and 1.563, respectively. N_{tr} is calculated as 1.6 by (21). The designed parameters are listed in Table II.

B. Implementation of LCC Resonant Converter with CWVM

By considering the CWVM capacitors from the proposed model, the resonant tank of LCC converter should be implemented. The designed parameters C_s and C_p are capacitors based on the transformer primary side, and C_{eqs} and C_{eqp} obtained by FW-CWVM are capacitors based on secondary side. From the designed FW-CWVM, C_{eqs} is calculated as 15.69nF by (14) and (15). Since the

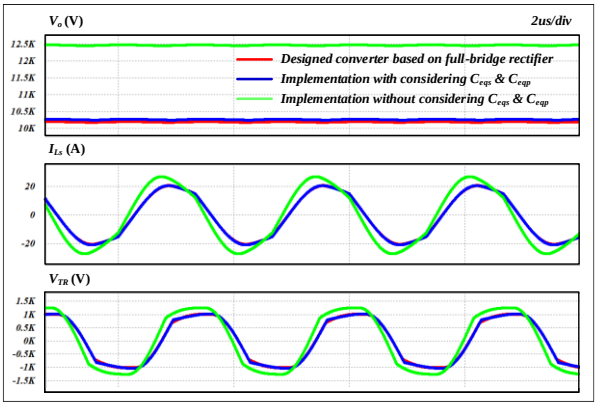

Fig. 6. Simulation results of designed and implemented LCC resonant converters.

junction capacitance of used diode (C5D05170H, CREE) for the FW-CWVM is about 40pF, C_{eqp} is obtained as 320pF by (11). The obtained C_{eqs} of 15.69nF can be utilized as C_s in the designed parameters because C_{eqs} reflected to the primary side of transformer is about 40nF. By considering C_{eqp} of 320pF, the capacitor of about 1.87nF is required in the transformer secondary side for C_p of 5.6nF. Thus, the capacitor of 2nF is connected to the FW-CWVM.

Fig. 6 shows the simulation results of designed and implemented LCC resonant converters. The red line is result of designed converter based on full-bridge rectifier. The blue line is the results of implemented converter with considering the equivalent capacitors and the green line is the results of implemented converter without considering the equivalent capacitors. The designed converter and implemented converter considering C_{eqs} and C_{eqp} can obtain the output voltage of about 10.2kV at the switching frequency of 375kHz and the root mean square (RMS) value of resonant current is estimated as 15A. However, the output voltage of converter without considering C_{eqs} and C_{eqp} is obtained as 12.5kV at the switching frequency of 375kHz and RMS current is about 19.1A. This indicates that there are large errors between the designed converter and implemented converter when C_{eqs} and C_{eqp} are neglected because the resonant tank is different.

IV. Experimental Results

To verify the proposed work, the experiments are performed by using the LCC resonant converter of 10kV and 5kW. Fig. 7 shows photograph of the experimental environment. The full-bridge inverter is implemented by SiC MOSFET (C3M0065090D, CREE) for the high switching frequency. The transformer leakage inductance is utilized as L_s. The resistor load of 20kΩ is used for the experiment.

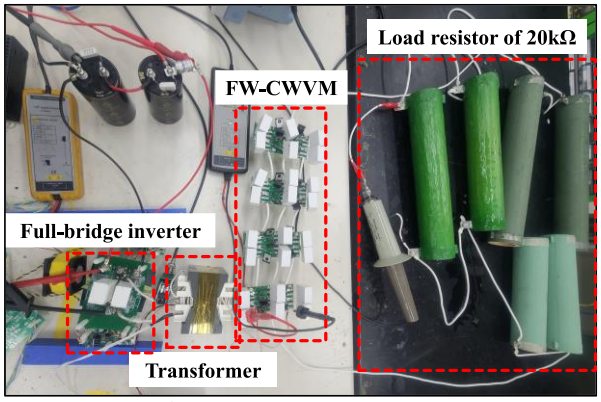

Fig. 7. Photograph of the experimental environment.

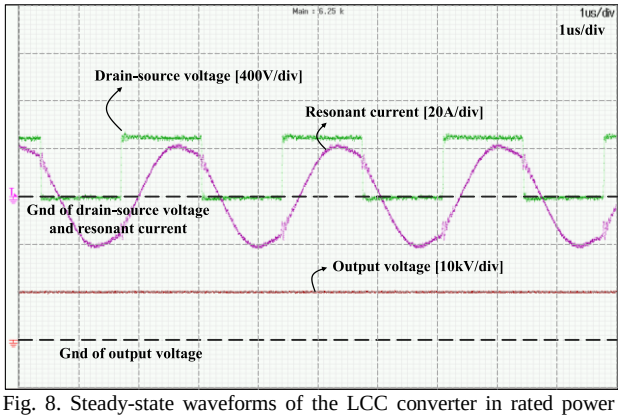

Fig. 8. Steady-state waveforms of the LCC converter in rated power operation (5kW).

Fig. 8 shows the steady-state waveforms of the LCC converter in rated power operation (5kW). The output voltage of 10kV is obtained at 374kHz. The RMS value of resonant current is measured as about 15A. These results are almost same to the simulation results of implemented LCC converter in Section III-B. The output voltage error between the results are estimated about 2%.

V. Conclusions

In this paper, a lumped parameter model of Cockcroft-Walton voltage multiplier (CWVM) is proposed for resonant converters with CWVM. It replaces the CWVMs with two lumped capacitors and ideal rectifiers. Through the proposed model, the resonance which occurs between CWVM capacitors and inductors of resonant inverter can be described with small error. The accuracy of proposed model is verified by PSIM simulation. The error between the actual circuit and proposed model is remarkably reduced compared with the conventional model. For the practical use of proposed model, the design and implementation of LCC resonant converter is presented. To confirm the feasibility of proposed lumped parameter model, the LCC resonant converter of 10kV and 5kW was built and the experiments for the rated power operation were performed. The output voltage error between the simulation and experimental results was measured as about 2%.

References

[1] Mohsen Ruzbehani, "A Comparative Study of Symmetrical Cockcroft-Walton Voltage Multipliers", Journal of Electrical and Computer Engineering, vol. 2017, Article ID 4805268,10 pages, 2017, doi: 10.1155/2017/4805268.

[2] B. Wu, S. Li, Y. Liu and K. Ma Smedley, "A New Hybrid Boosting Converter for Renewable Energy Applications," in IEEE Transactions on Power Electronics, vol. 31, no. 2, pp. 1203-1215, Feb. 2016, doi: 10.1109/TPEL.2015.2420994.I.S. Jacobs and C.P. Bean, "Fine particles, thin films and exchange anisotropy," *in Magnetism*, vol. III, G.T. Rado and H. Suhl, Eds. New York: Academic, 1963, pp. 271-350.

[3] X. Tang, Y. Xing, H. Wu and J. Zhao, "An Improved LLC Resonant Converter With Reconfigurable Hybrid Voltage Multiplier and PWM-Plus-PFM Hybrid Control for Wide Output Range Applications," in IEEE Transactions on Power Electronics, vol. 35, no. 1, pp. 185-197, Jan. 2020, doi: 10.1109/TPEL.2019.2914945.

[4] X. Tang, Y. Xing, H. Wu and J. Zhao, "An Improved LLC Resonant Converter With Reconfigurable Hybrid Voltage Multiplier and PWM-Plus-PFM Hybrid Control for Wide Output Range Applications," in IEEE Transactions on Power Electronics, vol. 35, no. 1, pp. 185-197, Jan. 2020, doi: 10.1109/TPEL.2019.2914945.

[5] H. Peng, J. Chen, Z. Cheng, Y. Kang, J. Wu and X. Chu, "Accuracy-Enhanced Miller Capacitor Modeling and Switching Performance Prediction for Efficient SiC Design in High-Frequency X-Ray High-Voltage Generators," in IEEE Journal of Emerging and Selected Topics in Power Electronics, vol. 8, no. 1, pp. 179-194, March 2020, doi: 10.1109/JESTPE.2019.2951743.

[6] S. Mao, C. Li, W. Li, J. Popović, S. Schröder and J. A. Ferreira, "Unified Equivalent Steady-State Circuit Model and Comprehensive Design of the LCC Resonant Converter for HV Generation Architectures," in IEEE Transactions on Power Electronics, vol. 33, no. 9, pp. 7531-7544, Sept. 2018, doi: 10.1109/TPEL.2017.2774147.

[7] S. -H. Son et al., "Development of 80-kW High-Voltage Power Supply for X-ray Generator," in IEEE Transactions on Industrial Electronics, vol. 70, no. 4, pp. 3652-3662, April 2023, doi: 10.1109/TIE.2022.3181363.
[8] J. S. Brugler, “Theoretical performance of voltage multiplier circuits,” IEEE J. Solid-State Circuits, vol. SC-6, no. 3, June 1971, pp. 132-135.
[9] L. Malesani and R. Piovan, "Theoretical performance of the capacitor-diode voltage multiplier fed by a current source," in IEEE Transactions on Power Electronics, vol. 8, no. 2, pp. 147-155, April 1993, doi: 10.1109/63.223966.
[10] Qian, Weijun. “Modeling and analysis of high frequency high voltage multiplier circuit for high voltage power supply.”, 2017.
[11] G. Ivensky, A. Kats and S. Ben-Yaakov, "An RC load model of parallel and series-parallel resonant DC-DC converters with capacitive output filter," in IEEE Transactions on Power Electronics, vol. 14, no. 3, pp. 515-521, May 1999, doi: 10.1109/63.761695.
[12] A. K. Rathore and V. R. Vakacharla, "A Simple Technique for Fundamental Harmonic Approximation Analysis in Parallel and Series–Parallel Resonant Converters," in IEEE Transactions on Industrial Electronics, vol. 67, no. 11, pp. 9963-9968, Nov. 2020, doi: 10.1109/TIE.2019.2952820.
[13]